Study of plastic hinge length in high-speed railway bridge piers

G. Shao & L. Jiang

School of Civil Engineering, Central South University, China

N. Chouw

Department of Civil and Environmental Engineering, The University of Auckland, New Zealand

2013 NZSEE Conference

ABSTRACT: Solid piers with rounded rectangular cross-section are widely used in China's high-speed railway bridges. These piers have high width-to-thickness ratio and less steel reinforcement. Plastic hinge length, L_p, is usually used in simplified design of piers under earthquake loading. Local engineers followed international seismic standards for designing these piers. These standards may not reflect the true behaviour of local prevailing conditions. Therefore, there is a need to develop a guideline for piers in China. As part of development process, nine large-scale specimens were tested and the results were used to study L_p. The experimental results matched well with the Chang-Mander concrete model. Thus, this model was further used to analyse the behaviour of piers with various parameters. The pier height and axial compression ratio are the most influencing factors for the development of L_p. Compared to available the design equations, the proposed equation predicted L_p well.

1 INTRODUCTION

Bridge piers can undergo elastic or plastic deformations depending upon the load intensity. Once the plastic deformation is reached, the plastic hinge is formed at the maximum moment region. The plastic region causes a dramatic increase in plastic curvatures near the base of the bridge pier. For simplicity, the plastic curvatures are usually assumed to be uniform over a height, called the plastic hinge length (Priestley 1987).

Plastic hinge length, L_p, can be used to predict the lateral load-drift response of columns. Researchers proposed empirical equations to estimate L_p and verified the developed equations using experimental results. The following factors considerably influence L_p: 1) the axial load; 2) moment gradient; 3) the shear stress in the plastic hinge region; 4) the amount, dimensions and mechanical properties of longitudinal and transverse reinforcement; and 5) the concrete strength (Bae 2008). The columns considered were mainly for highway-bridges or building structures.

Compared to highway-bridge columns, the design requirements of piers of the high-speed railway bridges are more complicated. These requirements include the high longitudinal and lateral stiffness, high pier width-to-thickness ratio and low longitudinal reinforcement ratio (Jia 2008). The highway-bridge columns and the high-speed railway bridge piers are referred, here-in-after, as highway columns and railway piers, respectively. The higher stiffness of railway piers are to satisfy the requirement of comfortable and stabling train movement (Zhu 2010).

Chinese guideline for seismic design of railway bridges has not given any suggestions on L_p. Therefore, to evaluate L_p of railway piers, nine large-scale specimens were tested under low cyclic loading. The experimental results were compared with the Chang-Mander concrete model (Waugh 2009) for validating the analytical approach. This approach was adopted to further analyse the behaviour of railway piers for the factors mentioned above. With the knowledge obtained from experimental and analytical results, a new equation is proposed for L_p of railway piers by the method of least squares fitting.

2 PLASTIC HINGE LENGTH AND PREVIOUS MODELS

2.1 *Definition of plastic hinge length*

The curvature distribution of section along the height of piers under earthquake loading is complex. However, in order to build a relation between the top displacement and the curvature of the plastic hinge region this can be simplified. Priestley and Park assumed that the curvatures of section are linear along the height of pier till the tensile reinforcements within plastic hinge region yield (Priestley 1987). After yielding, the curvatures grow dramatically in plastic hinge region and the curvatures above it remain same (as shown in Figure 1). The ultimate displacement Δ_u on the top of pier could be expressed as:

$$\Delta_u = \Delta_y + \Delta_p = \frac{1}{3}\phi_y L^2 + (\phi_u - \phi_y)L_p(L - 0.5L_p) \quad (1)$$

where Δ_y is the yield displacement on the top of pier; Δ_p is the plastic displacement; L is the height of pier; ϕ_y and ϕ_u are the yield curvature and the ultimate curvature, respectively; θ_p is the plastic rotation.

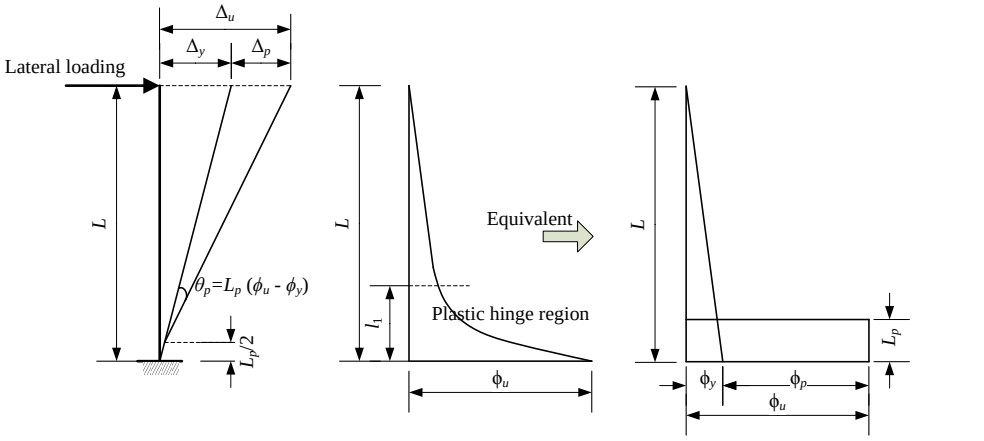

(a) Lateral displacement of pier (b) Theoretical curvature distribution (c) Equivalent curvature distribution

Figure 1. Definition of plastic hinge length

As shown in Equation (1), the displacement on the top of pier will be easily determined by the ultimate curvature, the yielding curvature and the plastic hinge length. By solving the Equation (1) L_p can be calculated as follows:

$$L_p = L - \sqrt{L^2 - 2A} \quad (2)$$

where, $A = (\Delta_u - \Delta_y) / (\phi_u - \phi_y)$.

2.2 *Previous empirical equations*

After carrying out the low-cyclic tests on reinforced concrete columns, Paulay and Priestley (1992) proposed the equation for the calculation of L_p in columns to account for the height of columns and different grades of flexural reinforcement. The expression is given in Equation (3).

$$L_p = 0.08L + 0.022 f_y d_s \quad (3)$$

where L is the height of column, d_s is the diameter of the longitudinal bars, f_y is the yielding strength of the longitudinal bars and the unit of the strength is MPa.

Based on this empirical equation, many international standards revised the expression of L_p for the various conditions. Caltrans seismic design criteria (Caltrans 2010) adopted the Equation (3) directly. Guidelines for seismic design of highway bridges in China (JTG/T B02-01) (MOT 2008) and Eurocode 8 (EN-1998 2005) made a slight modification. Seismic design specifications of highway bridges in Japan (JRA 2002) and New Zealand Standard NZS-3101:2006 (SNZ 2006) take into

account of the effect of the width of cross-section in loading direction on L_p. The empirical equations adopted in above mentioned design specifications are listed in Table 1. h is the width in the loading direction or the diameter of piers with circle cross section. h_e is the effective width of cross section. M^* and V^* are the design moment and shear action, respectively. When using Equations (4) and (7) the minimum L_p values should be used.

Table 1. L_p according to international standards

Standards	Plastic hinge length L_p	
Caltrans 2010	$0.08L + 0.022f_s d_s$	(3)
JTG/T B02-01	Minimum ($0.08L + 0.022f_s d_s \geq 0.044f_s d_s$ or $2/3h$)	(4)
Eurocode 8	$0.1L + 0.015f_s d_s$	(5)
JRA 2002	$0.2L - 0.1h$; $0.1h \leq L_p \leq 0.5h$	(6)
NZS-3101:2006	Minimum ($0.5h_e$ or $0.2M^*/V^*$) $\geq 0.5h_e$	(7)

Apart from the empirical equations in mentioned design specifications, many researchers have also put forward other L_p equations which take account of more factors. Sakai and Sheikh (1989), Bayrak and Sheikh (1998) and Mendis (2001) have successively given the equations based on testing members. In addation, Bae (2008) proposed a L_p expression including the depth of column, the area of tension reinforcement and the axial force. However, these equations have not been widely used for the design of piers.

3 METHODOLOGY

3.1 *Experimental procedures*

The cross sections of railway piers were scaled for laboratory tests because of actuator limitations. When the actual height of railway piers is up to 15m, the geometry scale of laboratory specimens is taken as 1:5. A scale of 1:8 is used when the height is 15-25 m. The cross-sections of the real piers (indicated as P1 and P2) and test specimens (named as S1 and S2) are shown in Figure 2. The indications of the cross-sections of piers and specimens are selected based on the pier height. A total of nine specimens were tested in three groups based on their heights i.e. 1.6, 2 and 3 m. The group with 1.6 m height has S1 while other groups have S2 cross-section.

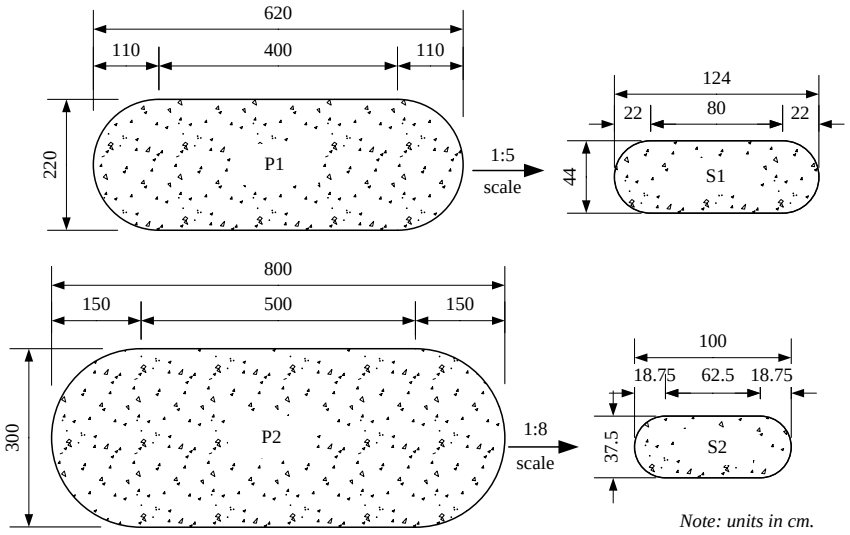

(a) Real piers (b) Test specimens

Figure 2. Dimensions of real piers and test specimens

Table 2. Factors and levels in test design

Factor/ variable	Level		
Height of specimens (m)	1.6	2	3
Axial compression ratio $N/(f_cA)$ (%)	5	10	15
Longitudinal reinforcement ratio ρ_s (%)	0.15	0.40	0.75
Volume-stirrup ratio ρ_v (%)	0.15	0.30	0.45

When the number of variables and levels for an experiment is relatively small, then the testing can be conducted with all possible combinations to completely understand the behaviour. But if the number of variables and levels are high, then it is difficult to consider all possible combinations. In this case, selected combinations are considered so that the experimental work can be performed conveniently without losing the understanding of the behaviour. The orthogonal array method (often referred to taguchi methods) is usually adopted for the selection of most influential combinations. Orthogonal array method can not only reduce the cost of experimental work but also improve the test efficiency because it reflects the representative coverage of all possible combinations. Orthogonal array should meet two requirements (Ji 2001): 1) to perform the same number of tests at any different levels for each variable; 2) to perform the same number of tests in level combination for any two factors. These two characteristics are called orthogonality which makes sure that the distribution of every variable and levels in tests can be uniform.

For an experiment which contains four variables and each variable has three levels, the possible combinations are 81, i.e. 3^4. For this case, the orthogonal method recommends an array of L_9 which means that a set of nine tests are required. The orthogonal array method is usually adopted for the selection of most influential combinations. There are there levels in each column which represents different variables and every level will be repeated three times. It is usually to arrange the array at random rather than rank each level in order of value (Ji 2001). The selected combinations of design parameters (taken from Table 2) are listed in Table 3.

Table 3. Design parameters in orthogonal tests on pier models

Model Number	SOL-1	SOL-2	SOL-3	SOL-6	SOL-8	SOL-9	SOL-11	SOL-12	SOL-13
Height (m)	1.6	1.6	1.6	2	2	2	3	3	3
$N/(f_cA)$**(%)**	15	5	10	5	15	10	10	15	5
ρ_s **(%)**	0.75	0.15	0.4	0.75	0.4	0.15	0.75	0.15	0.4
ρ_v**(%)**	0.3	0.45	0.15	0.15	0.45	0.3	0.45	0.15	0.3

The specimens were tested under low cyclic loading and the details are provided in (Jiang 2013). The force-displacement curves were obtained and their envelope is defined as the skeleton curve. The ultimate displacement is defined as the maximum displacement corresponding to the 85% of its maximum strength after the peak value. The experimental results of skeleton curves are used here for a comparison with that of analytical results in the following subsection.

3.2 *Analytical skeleton curves*

The structure can be simulated at three levels which are section level, three dimensional element level and fibre section level (Jiang 2005). At the section level, it requires the moment-curvature relation of the section. The simulation method is simple and produces a rough approximation. With the method of three dimensional element level, a large number of finite elements will be established and all parameters in the constitutive model need to be determined. Therefore, it will also take more computational space and time. The analysis might be difficult to converge. The fibre section method not only takes less time to analyse, it is also convenient to be implemented in a numerical model.

The fibre section method is applied to this analysis. Regarding the fact that two types of material are involved in each pier, the section can be discretized as accurate as possible. The patch fibre is used to represent the concrete fibres and individual fibres simulate the steel fibres. Subsequently, the uniaxial

stress-stain relation will be introduced to the fibres. The nodes of the individual fibre section elements associated to both materials are linked rigidly, i.e. for simplicity the bond-slip effect is not considered. An analytical model is shown in Figure 3 and the strains in fibre section are based on Euler–Bernoulli assumptions, i.e. plane sections remain plane.

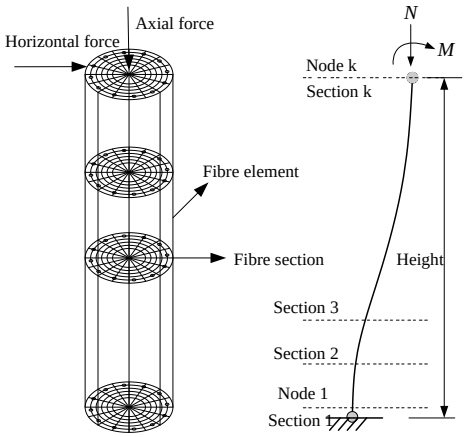

Figure 3. Analysis model at the fibre section level

Chang-Mander uniaxial model (Waugh 2009) and Giuffré-Menegotto-Pinto model (Filippou 1983) were used to simulate the behaviour of concrete and steel, respectively. Compared to other concrete models, Chang-Mander model takes into account more control factors, and energy-dissipation quantities, and it can simulate the narrow hysteretic loops of railway piers caused by less longitudinal reinforcement ratio (Jiang 2013). The software OpenSees developed at the University of California at Berkley was used to analyse the force-displacement of specimens using the detailed material parameters.

3.3 *Comparison between the experimental and analytical skeleton curves*

The experimental and analytical skeleton curves are compared in Figure 4. The analytical ultimate displacement is also defined as the maximum displacement corresponding to the 85% of its maximum strength after the peak value. The analytical peak loading force on the top of piers is slightly smaller than the experimental results, but both curves matched well as a whole. It shows that the adopted analytical method is relatively accurate for predicting the behaviour of the railway piers. Therefore, this method can be extended to analyse the other combinations of different variables and levels for parametric analysis.

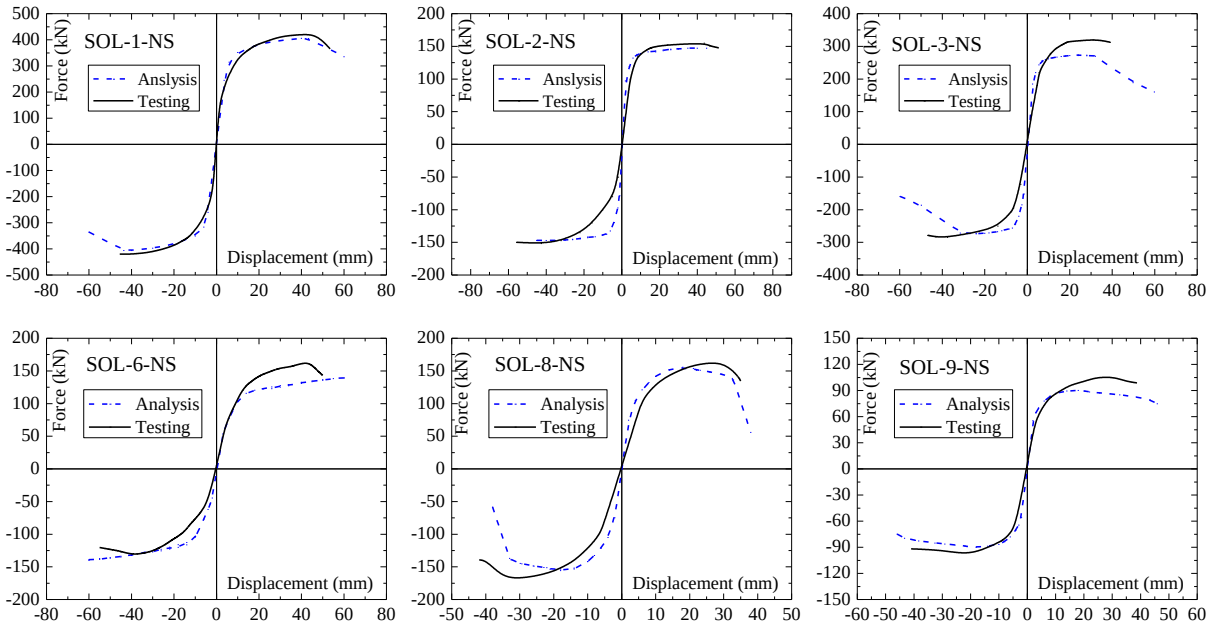

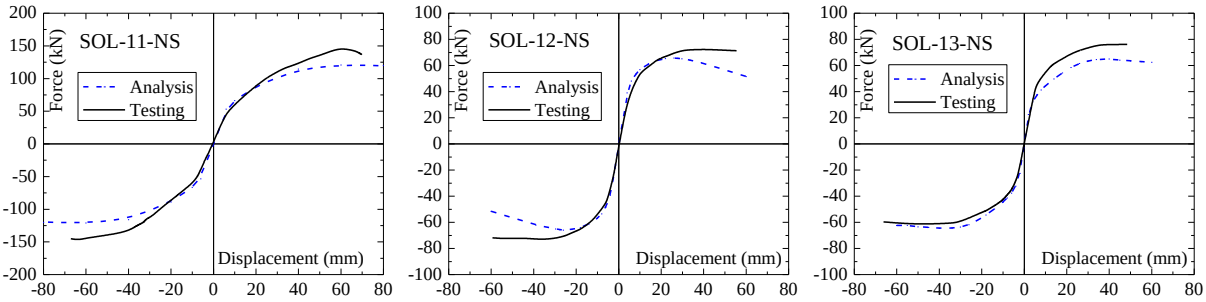

Figure 4. Analytical and experimental force displacement skeleton curves

4 PARAMETRIC ANALYSIS OF REAL PIERS

For L_p, the considered surplus parameters in addition to those mentioned in Table 2 are steel yield strength f_y and rebar diameter d_s. To ensure the same material cross-sectional property, the parameter ρ_v is kept constant and f_c of concrete is taken as 26 MPa for all cases in parametric analysis. Analytical parameters are listed in Table 4. In order to discuss the effect of cross-section on L_p, two cross sections in Figure 2 were considered. The cross-section P1 is adopted for piers mentioned at rows 1-15. Other piers at rows 16-19 have the cross-section P2. The variable parameters of the typical railway pier are made bold at row 2 in Table 4. For other piers, only the altered variables are in bold. For parametric analysis, the force-displacement and moment-curvature skeleton curves under the cyclic loading were obtained using the method explained in section 3.2 and finally analytical L_p was determined using Equation (2). For comparison purpose, L_p was also calculated from the equations given in Table 1.

Table 4. Parametric analysis and comparison of L_p

No.	Variable parameters					Analytical	Calculated L_p (m)				
	L (m)	ρ_s (%)	$N/(f_cA)$ (%)	f_y (MPa)	d_s (mm)	L_p (m)	Caltrans Eq. 3	JTG/T Eq. 4	Eurocode Eq. 5	JRA Eq. 6	NZS Eq.7
1	**6**	0.75	10	390	26	0.486	0.703	0.703	0.752	0.980	1.100
2	**10**	**0.75**	**10**	**390**	**26**	0.752	1.023	1.023	1.152	1.100	1.100
3	**14**	0.75	10	390	26	1.217	1.343	1.343	1.552	1.100	1.100
4	**18**	0.75	10	390	26	1.462	1.663	1.467	1.952	1.100	1.100
5	**22**	0.75	10	390	26	1.695	1.983	1.467	2.352	1.100	1.100
6	10	**0.50**	10	390	26	0.839	1.023	1.023	1.152	1.100	1.100
7	10	**1.00**	10	390	26	0.710	1.023	1.023	1.152	1.100	1.100
8	10	0.75	**5**	390	26	1.046	1.023	1.023	1.152	1.100	1.100
9	10	0.75	**15**	390	26	0.651	1.023	1.023	1.152	1.100	1.100
10	10	0.75	**20**	390	26	0.572	1.023	1.023	1.152	1.100	1.100
11	10	0.75	10	390	**22**	0.749	0.989	0.989	1.129	1.100	1.100
12	10	0.75	10	390	**30**	0.749	1.057	1.057	1.176	1.100	1.100
13	10	0.75	10	**350**	26	0.780	1.000	1.000	1.137	1.100	1.100
14	10	0.75	10	**440**	26	0.707	1.046	1.046	1.168	1.100	1.100
15	10	0.75	10	**500**	26	0.693	1.086	1.086	1.195	1.100	1.100
16	**10**	0.75	10	390	26	0.726	1.023	1.023	1.152	1.500	1.500
17	**14**	0.75	10	390	26	1.195	1.343	1.343	1.552	1.500	1.500
18	**18**	0.75	10	390	26	1.384	1.663	1.467	1.952	1.500	1.500
19	**22**	0.75	10	390	26	1.570	1.760	1.760	2.200	1.500	1.500

Note: Constant parameters are f_c =26 MPa *and* ρ_v = 0.45%.

It is observed from the analytical L_p in Table 4 that the height of piers and $N/(f_cA)$ have a larger influence on L_p compared to the other factors. The rebar diameter has the smallest influence. The analytical L_p increase linearly with the height of piers.

A comparison reveals that L_p calculated using previous Equations (3-7) do not match with the analytical values. The relationship between L_p and the most influencing factors L and $N/(f_cA)$ are shown in Figure 5. The results show that the analytical L_p are smaller than that of Caltrans, Eurocode 8 in piers with the same height, but larger than that of JRA and NZS when the height of piers is larger or equal to 18m. The analytical L_p decreases obviously with increasing axial compression ratio. However, L_p obtained from Equations (3-7) remains the same.

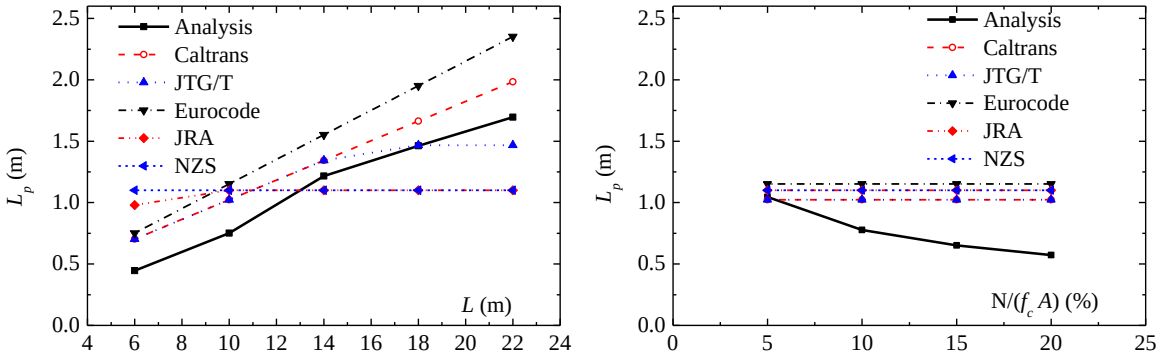

(a) L-L_p relationship (b) $N/(f_cA)$-L_p relationship

Figure 5. L_p dependency on the most influencing factors L and $N/(f_cA)$

Using the analytical L_p, a new equation is proposed by the method of least squares fitting considering the most influencing factors L and $N/(f_cA)$.

$$L_p = 0.073L - 2.64N/(f_cA) + 0.32 \quad (8)$$

A comparison between the analytical L_p and calculated L_p using the equation (8) with L and $N/(f_cA)$ are shown in Figure 6. As shown the bar graph, the new equation agrees well with the analytical L_p.

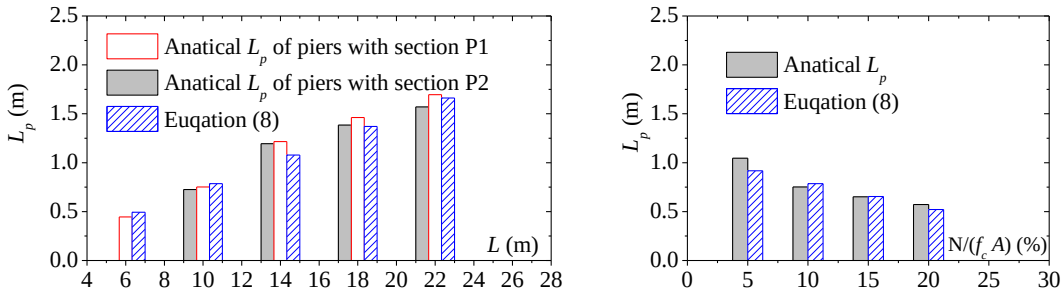

(a) L-L_p relationship (b) $N/(f_cA)$-L_p relationship

Figure 6. Verification of the proposed equation for L_p

5 CONCLUSIONS

Large scale experiments have been performed to investigate the plastic region of a RC bridge pier. From the force-displacement curves derived from the experimental results an equation for predicting the plastic length has been developed and compared with the existing equations defined in international standards. The research reveals:

1) Chang-Mander concrete model matched the experimental results well.

2) The pier height and axial compression ratio are the most influencing factors for the development of L_p.

3) Using the experimental results a new equation for L_p is proposed. It has the capability to predict L_p

more accurately.

ACKNOWLEDGEMENTS

The authors would like to thank the Ministry of Railways of China for the support of this research at National Engineering Laboratory for High Speed Railway Construction in China under contract number 2009G-024. The authors are also very grateful to the China Scholarship Council for the support of the first author's PhD research and stay at the University of Auckland. Constructive comments by Dr Majid Ali have improved the article.

REFERENCES

Bae, S. and Bayrak, O. 2008. Plastic hinge length of reinforced concrete columns. *ACI Structural Journal* 105(3): 290-300. Farmington Hills: American Concrete Institute.

Bayrak, O. and Sheikh, S.A. 1998. Confinement Reinforcement Design Considerations for Ductile HSC Columns. *Journal of Structural Engineering, ASCE*, 124(9): 999-1010.

Caltrans 2010. *Seismic Design Criteria Version 1.6*. Sacramento: California Department of Transportation.

EN-1998 2005. *Euro code 8: Design of structures for earthquake resistance-Part 2: Bridges*. Brussels: CEN (European Committee for Standardization).

Filippou, F.C. Popov, E.P. Bertero, V.V. 1983. *Effects of bond deterioration on hysteretic behaviour of reinforced concrete joints. Report UCB/EERC-83/19*. Berkeley: University of California, Berkeley.

Ji, Z.Y. 2001. *The method and theory of orthogonal design*. Hong Kong: Science and Technology across the World Press.

Jia, H.M. 2008. *Seismic performance of round end pier in passenger railway*. Beijing: Beijing Jiaotong University.

Jiang, J.J. Lu, X.Z. Ye, L.P. 2005. *Finite element analysis of concrete structures*. Beijing: Tsinghua University Press.

Jiang, L.Z. Shao, G.Q. Wang, H. Jiang, J.J. 2013. Experimental study on seismic performance of solid piers with round ended cross-section in high-speed railway. *China Civil Engineering Journal*. In print.

JRA 2002. *Specifications for highway bridges- Part V Seismic design*. Tokyo: Japan Road Association.

Ju, Y.Z. 2004. *Study on seismic performance of round-ended railway bridge piers with low longitudinal steel ratio*. Beijing: Beijing Jiaotong University.

Mendis, P. 2001. Plastic Hinge Lengths of Normal and High-Strength Concrete in Flexure. *Advances in Structural Engineering*, 4(4):189-195.

MOT (Ministry of Transport of the People's Republic of China) 2008. *Guidelines for seismic design of highway bridges (JTG/T B02-01)*. Beijing: China Communications Press.

Paulay, T. and Priestley, M.J.N. 1992. *Seismic design of reinforced concrete and masonry buildings*. New York: Wiley.

OpenSees (Open system for earthquake engineering simulation), http://opensees.berkeley.edu/.

Priestley, M.J.N. and Park, R. 1987. Strength of ductility of concrete bridge columns under seismic loading. *ACI Structural Journal* 84(1): 61-76. Farmington Hills: American Concrete Institute.

Sakai, K. and Sheikh, S.A. 1989. What Do We Know about Confinement in Reinforced Concrete Columns? (A Critical Review of Previous Work and Code Provisions). *ACI Structural Journal*, 86(2):192-207.

SNZ 2006. *Concrete Structure Standard, Part 1 - The Design of Concrete Structures (NZS 3101: Part 1: 2006)*. Wellington: Standards New Zealand.

Waugh, J.D. 2009. *Nonlinear Analysis of T-shaped Concrete Walls Subjected to Multi-directional Displacements*. Ames: Iowa State University.

Zhu, M. Yang, Y.Y. Chen, L. Bai, Q.C. He, T.G. 2010. Analysis on bridge pier design of Wuhan-Guangzhou railway passenger dedicated line. *Railway Standard Design* 1: 100-104 Beijing: China Railway Engineering Consulting Group Co. Ltd.